

7-22-2024

Molecular Mechanism of Bitter Taste Receptor Agonist-Mediated Relaxation of Airway Smooth Muscle

Stanley Conaway

Weiliang Huang

Miguel A. Hernandez-Lara

Maureen A. Kane

Raymond B. Penn

See next page for additional authors

Follow this and additional works at: <https://jdc.jefferson.edu/transmedfp>



Part of the [Medical Pharmacology Commons](#), and the [Translational Medical Research Commons](#)

[Let us know how access to this document benefits you](#)

This Article is brought to you for free and open access by the Jefferson Digital Commons. The Jefferson Digital Commons is a service of Thomas Jefferson University's [Center for Teaching and Learning \(CTL\)](#). The Commons is a showcase for Jefferson books and journals, peer-reviewed scholarly publications, unique historical collections from the University archives, and teaching tools. The Jefferson Digital Commons allows researchers and interested readers anywhere in the world to learn about and keep up to date with Jefferson scholarship. This article has been accepted for inclusion in Center for Translational Medicine Faculty Papers by an authorized administrator of the Jefferson Digital Commons. For more information, please contact: JeffersonDigitalCommons@jefferson.edu.

Authors

Stanley Conaway, Weiliang Huang, Miguel A. Hernandez-Lara, Maureen A. Kane, Raymond B. Penn, and Deepak A. Deshpande

RESEARCH ARTICLE

Molecular mechanism of bitter taste receptor agonist-mediated relaxation of airway smooth muscle

Stanley Conaway Jr¹  | Weiliang Huang²  | Miguel A. Hernandez-Lara¹  |
Maureen A. Kane²  | Raymond B. Penn¹  | Deepak A. Deshpande¹ 

¹Center for Translational Medicine, Jane and Leonard Korman Lung Center, Thomas Jefferson University, Philadelphia, Pennsylvania, USA

²Department of Pharmaceutical Sciences, School of Pharmacy, University of Maryland, Baltimore, Maryland, USA

Correspondence

Deepak A. Deshpande, Center for Translational Medicine, Thomas Jefferson University, Rm 543 JAH, 1020 Locust St, Philadelphia, PA 19107, USA.
Email: deepak.deshpande@jefferson.edu

Funding information

HHS | NIH | National Heart, Lung, and Blood Institute (NHLBI), Grant/Award Number: HL137030, HL137030-S1, HL146645 and HL150560; University of Maryland School of Pharmacy Mass Spectrometry Center, Grant/Award Number: SOP1841-IQB2014

Abstract

G-protein-coupled receptors (GPCRs) belonging to the type 2 taste receptors (TAS2Rs) family are predominantly present in taste cells to allow the perception of bitter-tasting compounds. TAS2Rs have also been shown to be expressed in human airway smooth muscle (ASM), and TAS2R agonists relax ASM cells and bronchodilate airways despite elevating intracellular calcium. This calcium “paradox” (calcium mediates *contraction* by pro-contractile Gq-coupled GPCRs) and the mechanisms by which TAS2R agonists relax ASM remain poorly understood. To gain insight into pro-relaxant mechanisms effected by TAS2Rs, we employed an unbiased phosphoproteomic approach involving dual-mass spectrometry to determine differences in the phosphorylation of contractile-related proteins in ASM following the stimulation of cells with TAS2R agonists, histamine (an agonist of the Gq-coupled H1 histamine receptor) or isoproterenol (an agonist of the Gs-coupled β_2 -adrenoceptor) alone or in combination. Our study identified differential phosphorylation of proteins regulating contraction, including A-kinase anchoring protein (AKAP)2, AKAP12, and RhoA guanine nucleotide exchange factor (ARHGEF)12. Subsequent signaling analyses revealed RhoA and the T853 residue on myosin light chain phosphatase (MYPT)1 as points of mechanistic divergence between TAS2R and Gs-coupled GPCR pathways. Unlike Gs-coupled receptor signaling, which inhibits histamine-induced myosin light chain (MLC)20 phosphorylation via protein kinase A (PKA)-dependent inhibition of intracellular calcium mobilization, HSP20 and ERK1/2 activity, TAS2Rs are shown to inhibit histamine-induced pMLC20 via inhibition of RhoA activity and MYPT1 phosphorylation at the T853 residue. These findings provide insight

Abbreviations: AKAP, A kinase anchoring protein; ARHGAP, RhoA GTPase-activating protein; ARHGEF, RhoA guanine nucleotide exchange factor; ASM, airway smooth muscle; Ca^{2+} , intracellular calcium; cAMP, cyclic adenosine monophosphate; DAG, diacylglycerol; FDR, false discovery rate; FRET, fluorescence resonance energy transfer; GPCR, G-protein coupled receptor; IP_3 , inositol trisphosphate; LATS, large tumour suppressor kinase; L-type, large conductance; MLC, myosin light chain; MYLK, myosin light chain kinase; MYPT, myosin light chain phosphatase; PKA, protein kinase A; PKC, protein kinase C; $PLC\beta$, phospholipase C beta; RBD, Rho-binding domain; RhoA, Ras homolog family member A; TAS2R, type 2 taste receptor; YAP, yes-associated protein; β_2AR , β_2 -adrenoceptor.

This is an open access article under the terms of the [Creative Commons Attribution-NonCommercial](https://creativecommons.org/licenses/by-nc/4.0/) License, which permits use, distribution and reproduction in any medium, provided the original work is properly cited and is not used for commercial purposes.

© 2024 The Author(s). *The FASEB Journal* published by Wiley Periodicals LLC on behalf of Federation of American Societies for Experimental Biology.

into the TAS2R signaling in ASM by defining a distinct signaling mechanism modulating inhibition of pMLC20 to relax contracted ASM.

KEYWORDS

airway smooth muscle, asthma, chloroquine, rho a, TAS2R

1 | INTRODUCTION

Over 300 million people worldwide are affected by bronchoconstrictive disorders such as asthma, and the burden of asthma continues to rise every year. Airway smooth muscle (ASM) hypersensitivity and hypercontraction contribute to the airway obstruction observed in asthma.^{1,2} Although significant strides have been made in developing biologics for asthma management, approximately 50% of asthmatics have suboptimal control and are unable to reliably control bronchoconstriction with current bronchodilator drugs, including β_2 -adrenoceptor (β_2 AR) agonists.^{3–5} Therefore, there is a pressing need to develop newer and better bronchodilator therapies for treating asthmatics.

GPCRs expressed on ASM are the primary target for treating airway hyperresponsiveness in bronchoconstrictive disorders. ASM contraction and relaxation are regulated by Gq- and Gs-coupled GPCRs, respectively. Activation of Gq signaling in ASM leads to phospholipase C beta (PLC β)-dependent production of inositol triphosphate (IP₃) and diacylglycerol (DAG), release of intracellular calcium (Ca²⁺) through IP₃ receptor channels into the cytosol by IP₃ and activation of protein kinase C (PKC) by DAG. Collectively, Ca²⁺- and PKC-dependent signaling converge to increase MLC20 phosphorylation and facilitate actin–myosin cross-bridge cycling and ASM contraction.⁶ Activation of the Gs-coupled GPCRs results in the elevation of cAMP levels and activation of cAMP-dependent PKA, which phosphorylates various targets and attenuates Ca²⁺ mobilization, resulting in inhibition of contraction⁷; however, the extent to which PKC and Ras homolog family member A (RhoA)-related effectors are mediated by Gs-coupled signaling is not fully understood.

During an effort to screen for known and novel GPCRs in human ASM, the expression of type 2 taste receptors (TAS2Rs) was unexpectedly discovered.⁸ While TAS2Rs are predominantly expressed in taste cells, recent studies have demonstrated extra-gustatory expression and functions of TAS2Rs.^{8–13} We subsequently demonstrated that a variety of TAS2R agonists cause ASM relaxation and bronchodilation in a G-protein- $\beta\gamma$ -, PLC β -, and IP₃-mediated fashion, independent of PKA signaling.¹² ASM relaxation was observed with TAS2R compounds in ASM cells and airway tissues obtained from human, murine, and guinea pig lungs.^{14–19} Interestingly, whereas bitter tastants evoke

an elevation in Ca²⁺ mobilization when stimulated by themselves, bitter tastants are able to reduce the Ca²⁺ mobilization induced by Gq-coupled GPCR agonists.^{16,19–21} However, independent studies also suggest that TAS2R agonists evoke relaxation independently of compartmentalized Ca²⁺ signaling, possibly via G-protein- $\beta\gamma$ -mediated inhibition of Ca²⁺ flux through the large conductance (L-type) voltage-dependent calcium channels and/or IP₃ receptors.^{16,19} Collectively, these studies implicate distinct mechanisms employed by TAS2Rs and Gs-coupled GPCRs in regulating ASM contraction, likely involving compartmentalization of Ca²⁺ signaling and differential regulation of pro-contractile signaling elements to decrease ASM sensitization to Ca²⁺.

Accordingly, we undertook an unbiased analysis of ASM phosphoprotein regulation to gain insight into the differences by which agonists of TAS2Rs and Gs-coupled GPCRs regulate pro-contractile signaling. Having identified differentially regulated phosphoproteins linked to control of MLC20 phosphorylation (a key event in ASM contraction), we subsequently characterized the relevant pathways in biochemical analyses employing western blotting and fluorescence reporter assays, as well as imaging analyses to visualize spatiotemporal regulation of key regulators. We found that unlike Gs-coupled receptor signaling, which inhibits MLC20 phosphorylation via PKA-dependent inhibition of Ca²⁺ mobilization, HSP20 and ERK1/2 activity, TAS2Rs are shown to inhibit pMLC20 via inhibition of Ca²⁺ mobilization, RhoA activity, and MYPT1 phosphorylation at the T853 residue. Collectively, these findings provide insight into the TAS2R signaling paradox by defining a distinct compartmentalized signaling mechanism inhibiting pMLC20 to relax contracted ASM.

2 | MATERIALS AND METHODS

2.1 | Reagents

Chloroquine (C2301) was purchased from TCI (Portland, Oregon, USA). Anti- β -actin (58522) antibody, isoproterenol, flufenamic acid, and histamine were from Sigma Aldrich (St. Louis, MO, USA). Puromycin (1113803), DPBS (SH30028.02), fetal bovine serum (A3840101), insulin–transferrin–selenium–ethanolamine (41400), HEPES

(SH30237.01), NaOH (BP359-12) HBSS (14025), DMEM (11-995-73), L-glutamine (25030), F-12 nutrient mixture (11765-054), and 0.05% trypsin-EDTA (25300) were from Thermo Fisher Scientific (Waltham, MA, USA). The pLentiRhoA2G plasmid ([RRID:Addgene_40179](#)) was obtained from Addgene (Watertown, MA, USA). RhoA pull-down activation assay kit (BK036) and RhoA-specific monoclonal mouse antibody (ARH03, [RRID:AB_10708069](#)) were from Cytoskeleton (Denver, CO, USA). The phospho-RhoA (Ser188) rabbit antibody (41435, [RRID:AB_777708](#)) was from Abcam (Waltham, MA, USA). The phospho-PKC substrate antibody (6967, [RRID:AB_10949977](#)), phospho-MYPT1 (Thr696) polyclonal rabbit antibody (5163, [RRID:AB_10691830](#)), phospho-MYPT1 (Thr853) polyclonal rabbit antibody (4563, [RRID:AB_1031185](#)), and phospho-MLC polyclonal rabbit antibody (3674, [RRID:AB_2147464](#)) were from Cell Signaling Technology (Beverly, MA, USA). Secondary antibodies were from LICOR Biosciences (Lincoln, NE, USA).

2.2 | Cell culture

All studies involving human ASM cells were approved by Thomas Jefferson University's Institutional Review Board. Primary human ASM cells were isolated from healthy human donor lung tissue and grown in culture dishes in F-12 ASM growth media supplemented with HEPES (21.6 mM), NaOH (10.4 mM), L-glutamine (1.7 mM), penicillin (86.3 U/mL), streptomycin (86.3 µg/mL), CaCl₂ (1.5 mM), and fetal bovine serum (10% v/v) as described previously.^{22,23} Primary human ASM cells were grown to confluency, harvested with trypsin, and sub-cultured into new dishes. Following 80–90% confluency, cells were washed with DPBS and serum-starved for 3–5 days in ASM cell starvation media consisting of F-12 media supplemented with insulin, transferrin, selenium, and ethanolamine as previously described.²⁴

2.3 | Phosphoproteomic analysis

Starvation media were replaced with HBSS and human ASM cells were left undisturbed for 1 h prior to agonist treatment. Healthy ASM cells were treated with 1 µM isoproterenol, 300 µM chloroquine, or 10 µM histamine for 30 min. In addition, ASM cells were pretreated for 5 min with isoproterenol or chloroquine followed by treatment with histamine in order to assess the ability of chloroquine and isoproterenol to regulate the signaling elicited by histamine. Cells were harvested in RIPA buffer containing protease inhibitors and processed further for phosphoproteomic analysis. Briefly, in order to determine the phosphorylation

status of contractile-related signaling components, a global immunoprecipitation using titanium dioxide-coated beads with an affinity for phosphorylated tyrosine, threonine, and serine residues was performed on ASM lysates. Tryptic peptides were separated by a nanoACQUITY UPLC analytical column on a Waters nano-ACQUITY UPLC system and analyzed with a coupled Thermo Scientific Orbitrap Fusion Lumos Tribrid mass spectrometer as described previously.²⁵ Tandem mass spectra were searched against a UniProt reference human proteome. Carbamidomethylation of cysteine was treated as static modification. Phosphorylation of serine, threonine, and tyrosine, and deamidation of asparagine and glutamine were treated as dynamic modifications. Resulting hits were validated at a maximum global false discovery rate (FDR) of 0.01. The abundances of proteins were obtained by label-free quantitation.

2.4 | RhoA pull-down assay

ASM cells were treated with 1 µM isoproterenol, 300 µM chloroquine, or 10 µM histamine for 3 min in HBSS. In addition, ASM cells were pretreated for 15 min with isoproterenol or chloroquine followed by a 3-min treatment with histamine. Cell lysates were collected in RIPA buffer. In the pull-down assay, RhoA was selectively isolated in its active, GTP-bound form from the lysates of ASM cells using a GST-tagged Rhotekin RhoA-binding domain conjugated to agarose beads.^{26–28} Total ASM cell lysate and RhoA pull-down samples were run on an SDS-PAGE gel and assessed by western blot using a RhoA monoclonal mouse antibody (1:500 dilution) and LICOR secondary antibodies (1:25000 dilution). Densitometry was performed using the Odyssey Infrared Imaging System. The levels of active RhoA were then normalized to the amount of total RhoA for each treatment condition.

2.5 | Preparation of pLentiRhoA2G stable cell lines

A single-chain fluorescence resonance energy transfer (FRET) DNA construct containing a RhoA biosensor with dual-fluorescence (Venus and m-Turquoise fluorescent proteins) was used to measure RhoA activity. Lentivirus containing the RhoA2G vector was generated and processed as previously described (with slight modifications).^{29,30} Primary ASM cells were grown to 60–70% confluency in a 10-cm dish, washed, and fed 3 mL of ASM cell growth media (without pen/strep) 15 min prior to viral transduction. pLentiRhoA2G virus was dispersed dropwise evenly across the dish followed by overnight incubation. Next day, the media were replaced with complete

ASM cell growth media. After 72 h, transfection efficiency was confirmed by fluorescence imaging using an EVOS microscope. Fresh ASM cell growth media (with 2 mg/mL puromycin) were added to the dish for selection.

2.6 | Confocal microscopic imaging and data analysis

The pLentiRhoA2G stable lines were plated into 35-mm glass bottom MatTek dishes, mounted on a confocal microscope platform, and connected to a perfusion system. Cells were excited with a laser at 445 nm and emission spectra for inactive (Venus/488 nm) and active RhoA (FRET/535 nm) were determined. Images were acquired using a Nikon confocal microscope. Image J software was used to analyze the images. The FRET image, having the best signal-to-noise ratio, was designated as a reference to create a binary mask with a value of one inside the cell and a value of zero outside the cell for all images. Image spectra were then background-corrected and the adjusted FRET image was divided by the CFP image to obtain a ratio image representing RhoA activity at each timepoint as previously described.^{29,31} Ratio values were normalized using basal values (vehicle-treated cells) and a linear pseudocolor lookup table was applied to each image for qualitative purposes. Ratio images are color-coded, where high and low biosensor activity corresponds with warm (red) and cold (blue) colors, respectively.

2.7 | Western blot analysis

ASM cell lysates obtained in RIPA buffer containing protease inhibitors and reduced with NU-PAGE SDS sample buffer were processed as described previously.^{32–34} The cell lysates were separated on a SDS-PAGE gel and transferred onto a nitrocellulose membrane. The western blot membranes were incubated overnight at 4°C in tris-buffered saline containing Tween 20 (including 3% BSA) with antibodies (1:1000 dilution) specific for phospho-MLC, phospho-PKC substrates, phospho-RhoA (Ser188), phospho-MYPT1 (Thr696), and phospho-MYPT1 (Thr853). Densitometry was performed using the Odyssey Infrared Imaging System. The levels of p-MLC, p-PKC substrates, p-RhoA (Ser188), p-MYPT1 (Thr696), and p-MYPT1 (Thr853) were normalized using the intensities of β -actin for each sample.

2.8 | Statistical analysis

Statistical significance was determined using a one-way ANOVA followed by Tukey's *post-hoc* analysis using

GraphPad Prism version 9.5. The data represent the mean \pm S.E.M from n number of experiments where n represents an ASM culture obtained from an independent donor.

3 | RESULTS

3.1 | Contractile-related proteins are differentially phosphorylated by TAS2R agonists

Previous studies suggest that TAS2R activation attenuates MLC20 phosphorylation; however, the regulators upstream of MLC20 that are activated by TAS2R agonists are not established. In order to assess the phosphorylation of effectors in ASM cells induced by stimulating cells with TAS2R agonists in an unbiased manner, we employed a phosphoproteomic approach using mass spectrometry. ASM cells were treated with the TAS2R agonist chloroquine (300 μ M) or β_2 -agonist isoproterenol (1 μ M), alone or in combination with the bronchoconstrictive agonist histamine (10 μ M). Changes in the phosphorylation of cellular proteins were assessed by mass spectrometry. Our findings identified the percentage of differentially phosphorylated proteins compared to all related proteins within each of the G $\beta\gamma$, PLC β , RhoA, actin cytoskeleton, Hippo, and 14-3-3 signaling pathways upon treatment of cells with histamine alone or in tandem with isoproterenol or chloroquine (Figure 1A). The degree of phosphorylation-related perturbation in any given signaling pathway was reflected by taking the decadic logarithm (log base 10) of its corresponding p-value in the analyzed dataset. Signaling pathways with a transformed p-value greater than ± 1.3 (i.e., $p < .05$) were considered during the analysis (Figure 1B). A full list of proteins phosphorylated upon agonist stimulation of ASM cells is given in the Supplemental data (Table S1; A – Histamine, B – Chloroquine, C – Chloro+Hist, D – Isoproterenol, E – Isoproterenol+Hist). Contractile-related proteins within these pathway-specific clustered datasets were then investigated to determine differences relevant to the Gq, Gs, and TAS2R signaling pathways. Furthermore, phosphorylation of individual proteins within each pathway was measured using arbitrary units of abundance and the fold change in the abundance of phosphorylated proteins was obtained by dividing the abundance unit value of each treatment condition by that of the vehicle-treated condition (Figure 2).

Previous work from our group suggests that TAS2Rs elicit ASM relaxation in a PLC β -dependent manner.¹² PKC and RhoA are two important contractile-related proteins that are downstream of PLC β . Interestingly, the proteins that exhibited the most significant levels of change in their phosphorylation profiles were PKC-related proteins. We observed 2-fold and 2.5-fold increases in phosphorylation of

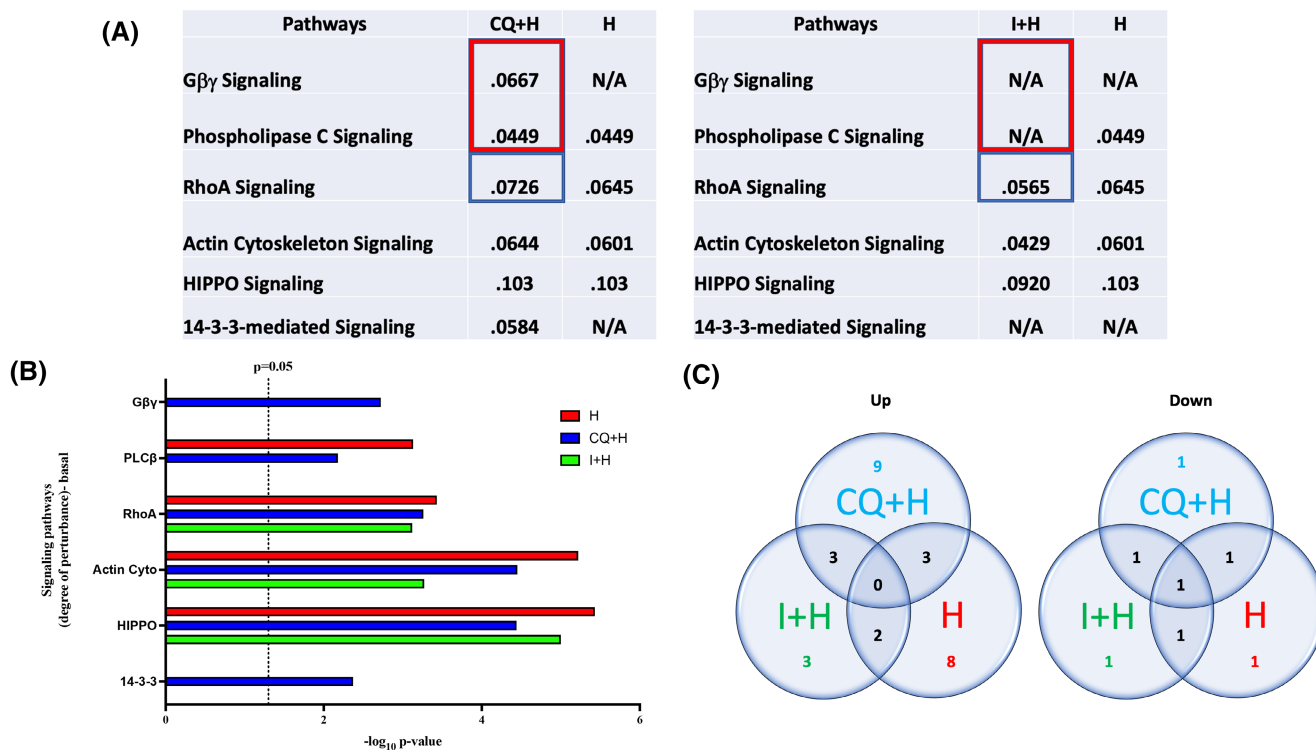


FIGURE 1 Agonist-specific differences of phosphorylated proteins in multiple signaling pathways. Phosphoproteomic analysis was performed on ASM cells to determine the profile for all proteins phosphorylated at serine, tyrosine, and threonine residues within the cell proteome. (A) Numerical values correspond to the percentage of proteins observed to be differentially phosphorylated in each respective signaling pathway following stimulation with 10 μ M histamine (H) or dual agonist treatment (300 μ M chloroquine: CQ + H and 1 μ M isoproterenol: I + H). Pathways that showed no significant change in treatment versus control conditions are denoted as N/A ($n=3$). (B) The degree of perturbation within each signaling pathway with respect to treatment condition as denoted by a negative \log_{10} transformation of the p-value. Pathways with transformed p-values greater than 1.3 ($p < .05$) were determined to be significantly perturbed. (C) Quantification of the number of contractile-related proteins that were differentially regulated between treatment conditions. $p < .05$ versus control.

the structural domain of AKAP2 and the PKC-binding domain of AKAP12 in histamine-treated ASM cells compared to vehicle-treated ASM cells, respectively. Conversely, we observed no change in phosphorylation of these proteins in ASM cells treated with isoproterenol or chloroquine compared to vehicle-treated cells (Figure 2A,B). Interestingly, pretreatment with isoproterenol led to decreased histamine-induced phosphorylation of AKAP2 and AKAP12, whereas chloroquine increased histamine-induced AKAP2 and AKAP12 phosphorylation.

We observed a 4-fold increase in phosphorylation of ARHGEF12 and no change in the phosphorylation of RhoA GTPase-activating protein (ARHGAP)6 in samples treated with histamine compared to vehicle-treated ASM cells (Figure 2C,D). Conversely, we observed no change in phosphorylation of ARHGEF12 and increased phosphorylation of ARHGAP6 in ASM cells treated with isoproterenol or chloroquine. Interestingly, pretreatment with isoproterenol or chloroquine did not significantly increase phosphorylation of ARHGAP6 in the presence of histamine; however, both agonists appeared to significantly attenuate histamine-induced phosphorylation of ARHGEF12.

Increased phosphorylation of AKAP12 and decreased phosphorylation of ARHGEF12 in the presence of chloroquine/histamine dual-treatment suggests that chloroquine mediates histamine-induced changes in a PKC- and RhoA-dependent manner. There were no significant changes in the phosphorylation of MYPT1, which suggests that upstream differences in PKC and RhoA phosphorylation may play an important role in TAS2R-mediated signaling in human ASM (Figure 2E,F). Additional pathway-specific phosphorylation of proteins is given in the Supplemental data (Table S2).

3.2 | Histamine-induced MLC phosphorylation is attenuated following treatment with TAS2R agonists

ASM contraction by GPCR agonists is preceded by MLC20 phosphorylation and is mediated via Ca^{2+} -dependent activation of myosin light-chain kinase (MYLK) or inhibition of MYPT1.^{35,36} In these studies, we assessed the effect of TAS2R agonists and isoproterenol

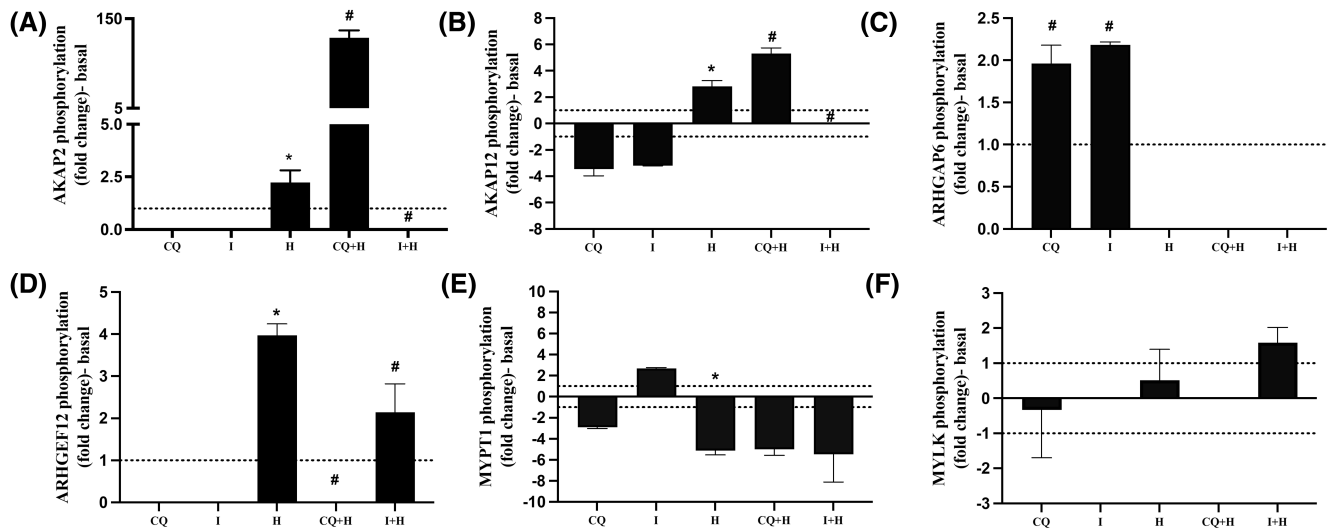


FIGURE 2 Agonist-specific differences of individual phosphorylated proteins of interest. Above are representative graphs of contractile-related proteins of interest compiled from our phosphoproteomic analysis: (A) AKAP2, (B) AKAP12, (C) ARHGAP6, (D) ARHGEF12, (E) MYPT1, and (F) MYLK. ASM cells were treated with 1 μ M isoproterenol (I), 300 μ M chloroquine (CQ), 10 μ M histamine (H), or dual agonist treatment (I+H and CQ+H) prior to phosphoproteomic analysis. Fold change is relative to non-treated control samples and increases/decreases in phosphorylation correspond with positive and negative fold changes ($n=3$). * $p < .05$ versus basal and # $p < .05$ versus histamine alone. Data were analyzed using a one-way ANOVA and are represented as mean \pm SEM.

on basal and histamine-induced MLC20 phosphorylation. As expected, histamine stimulation of ASM cells resulted in an increase in MLC20 phosphorylation. On the contrary, treatment with β_2 AR agonist isoproterenol (1 μ M) or TAS2R agonists chloroquine (300 μ M and 1 mM) and flufenamic acid (30 μ M and 300 μ M) alone did not induce MLC20 phosphorylation. When cells were treated concomitantly in the presence of histamine, the agonists chloroquine, flufenamic acid, and isoproterenol significantly reduced histamine-mediated MLC20 phosphorylation (Figure 3A,B). Furthermore, ASM cells pretreated with isoproterenol, chloroquine (300 μ M or 1 mM), or flufenamic acid (30 μ M or 300 μ M) displayed decreases in histamine-induced MLC20 phosphorylation by 4-, 3.3-, 3.6-, 3.8-, and 5.3-fold, respectively.

3.3 | PKC is differentially regulated by TAS2R agonists in ASM

PLC β is a common effector which is activated within the TAS2R and Gq signaling pathways; however, the differences in the regulation of proteins downstream of PLC β between these GPCR pathways remain to be elucidated.¹² Therefore, to evaluate and validate the findings from the phosphoproteomic data, levels of PKC activity were measured in ASM cells treated with isoproterenol (1 μ M), chloroquine (300 μ M and 1 mM), or flufenamic acid (30 μ M and 300 μ M) alone, or in combination with histamine (10 μ M) using an immunoblot assay that determines

phosphorylation of PKC substrates. We observed differences in phosphorylation of a PKC substrate between ~66 and 70 kDa in molecular weight. Histamine-induced phosphorylation of this PKC substrate is up to 6-fold higher than baseline levels. Chloroquine (300 μ M) and flufenamic acid increased the phosphorylation of this substrate above baseline levels by at least 1.5-fold compared to no induction with isoproterenol (Figure 4A,B). Furthermore, isoproterenol pretreatment reduced histamine-mediated PKC phosphorylation of substrates in this molecular weight range by 1.5-fold, while chloroquine and flufenamic acid (300 μ M) pretreatments produced a 3-fold reduction in signal. These findings are consistent with our previous work suggesting that TAS2R signaling is mediated in a PLC β -related manner while also highlighting counter-regulation of histamine-mediated PKC activation by chloroquine and flufenamic acid. Importantly, these findings also demonstrate the disparity between bitter tastants and isoproterenol in the regulation of histamine-mediated PKC activity in ASM cells.

3.4 | RhoA is differentially regulated across GPCR pathways in ASM cells

RhoA, which is a major PKC effector protein important for contraction, is activated by ARHGEFs and inhibited by ARHGAPs.³⁷⁻³⁹ Therefore, to evaluate the findings from the phosphoproteomic data regarding ARHGEF12 and ARHGAP6, levels of GTP-bound (active) RhoA were measured in ASM cells transduced with lentiviral particles

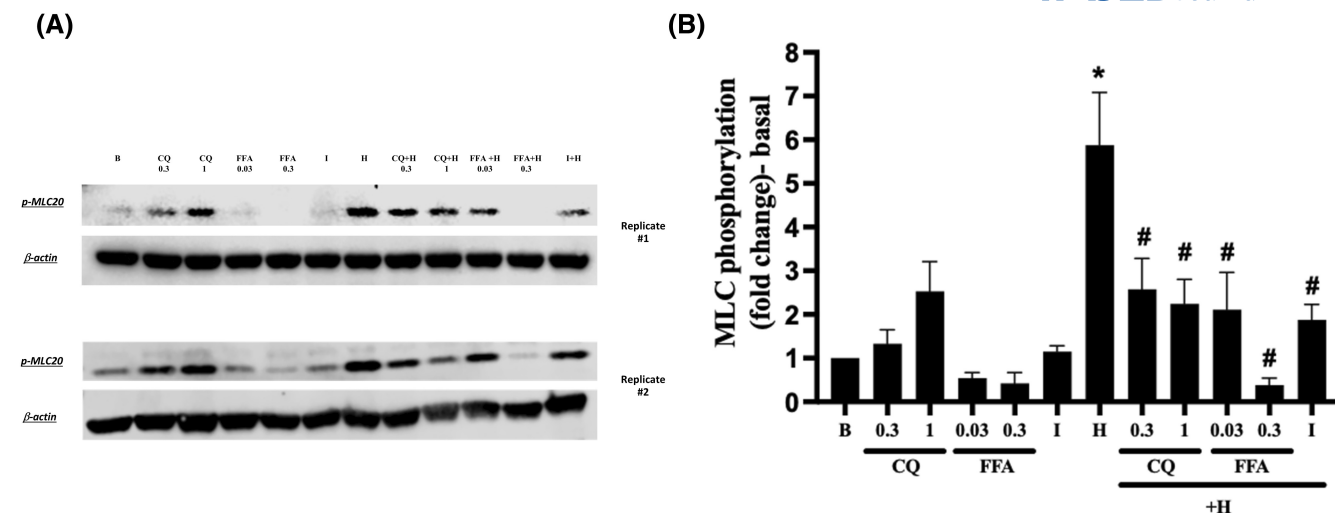


FIGURE 3 MLC20 is negatively regulated by TAS2R and β_2 AR pathways. The phosphorylation of MLC20 was measured in ASM cells treated with 1 μ M isoproterenol (I), 300 μ M or 1 mM chloroquine (CQ), 30 μ M or 300 μ M flufenamic acid (FFA), 10 μ M histamine (H), or dual agonist treatment (I+H, CQ+H or FFA+H). (A) Representative western blots of phosphorylated MLC20 in agonist-stimulated ASM cells. (B) Graph depicting the level of MLC20 phosphorylation normalized to β -Actin in each sample ($n=5-8$). * $p < .05$ versus basal and # $p < .05$ versus histamine alone. Data were analyzed using a one-way ANOVA and are represented as mean \pm SEM.

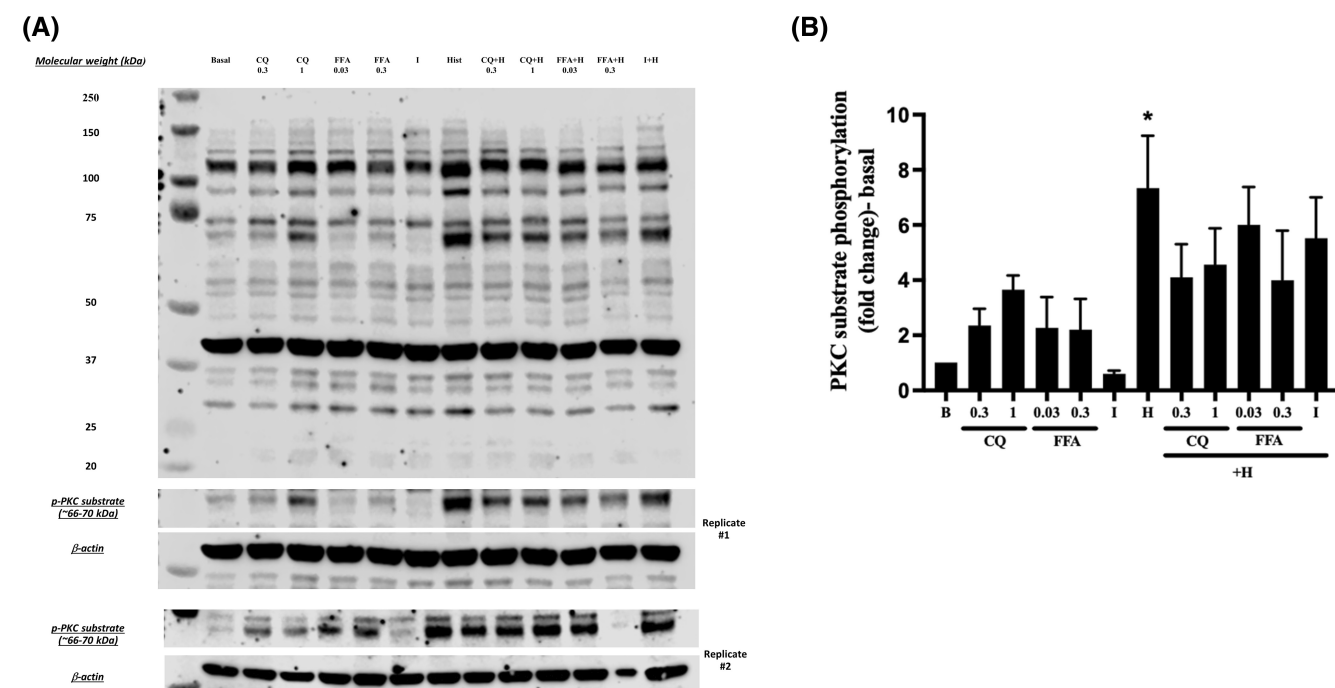


FIGURE 4 PKC may be differentially regulated by TAS2R and β_2 AR agonists. (A) The phosphorylation of PKC substrates was measured in ASM cells treated with 1 μ M isoproterenol (I), 300 μ M or 1 mM chloroquine (CQ), 30 μ M or 300 μ M flufenamic acid (FFA), 10 μ M histamine (H) or dual agonist treatment (I+H, CQ+H or FFA+H). (A) Representative western blot of phosphorylated PKC substrates normalized to β -Actin in each sample. (B) Representative graph of the amount of a 66–70 kDa phosphorylated PKC substrate normalized to β -Actin in agonist-stimulated ASM cells ($n=3-5$). * $p < .05$ versus basal. Data were analyzed using a one-way ANOVA and are represented as mean \pm SEM.

containing a single chain FRET⁴⁰ biosensor construct comprising RhoA and a Rho-binding domain (RBD) specific for GTP-bound RhoA. HBSS solution containing isoproterenol (1 μ M), chloroquine (300 μ M–1 mM), or flufenamic acid (300–700 μ M) alone was perfused onto ASM cells for 15 min

followed by perfusion with dual-treatment including histamine (10 μ M). Histamine treatment induced RhoA activation as expected. Interestingly, chloroquine, isoproterenol, and flufenamic acid pretreatment significantly attenuated histamine-induced RhoA activation (Figure 5A,B). However,

isoproterenol only partially attenuated histamine-induced RhoA activation, whereas chloroquine and flufenamic acid eliminated this response. Furthermore, there were noticeable differences in the spatial distribution of active RhoA across treatment conditions. An increase in fluorescent intensity near the nucleus and diffusion of active RhoA to the periphery was observed in ASM cells treated with histamine. Interestingly, ASM cells pretreated with chloroquine and flufenamic acid not only prevented histamine-mediated RhoA activation and diffusion but also resulted in the diffusion of active RhoA away from the cell periphery and closer to the nucleus (Figure 5C). We employed a pull-down assay to further validate the findings from fluorescence imaging. We observed a 2.5-fold increase in RhoA activation following treatment of ASM cells with histamine, while no significant RhoA activity was observed in cells treated with isoproterenol or chloroquine. Moreover, pretreatment with chloroquine (300 μ M) significantly attenuated histamine-induced RhoA activation, whereas there was only partial attenuation with isoproterenol (Figure 5D).

Isoproterenol and chloroquine both inhibited RhoA activation despite differences in the regulation of PKC, an upstream activator of RhoA. Therefore, we sought to establish the molecular differences, if any, in RhoA

regulation by isoproterenol and bitter tastants. Previous literature suggests that PKA-mediated phosphorylation of RhoA at the S188 amino acid residue increases the affinity of RhoA-GTP for the Rho guanine nucleotide dissociation inhibitor, which traditionally sequesters GDP-bound RhoA from the plasma membrane to the cytosol and maintains RhoA in an inactive state.^{41–43} Additionally, this phosphorylation event protects RhoA from ubiquitin-mediated degradation in the proteasome.⁴³ Our findings suggest that isoproterenol indeed facilitates phosphorylation of RhoA at S188 while chloroquine and flufenamic acid do not. Moreover, histamine also induced significant phosphorylation of RhoA at S188 alone, or in the presence of chloroquine and isoproterenol. Interestingly, pretreatment with flufenamic acid (300 μ M) significantly attenuated histamine-mediated phosphorylation at S188 (Figure 5E). These findings suggest that RhoA activity is inhibited canonically by bitter tastants, whereas isoproterenol treatment partially inhibits RhoA activity canonically and regulates RhoA non-canonically via S188 phosphorylation. Furthermore, the data suggest that regulation of histamine-mediated S188 phosphorylation is TAS2R agonist specific as flufenamic acid, not chloroquine, completely attenuated this response.

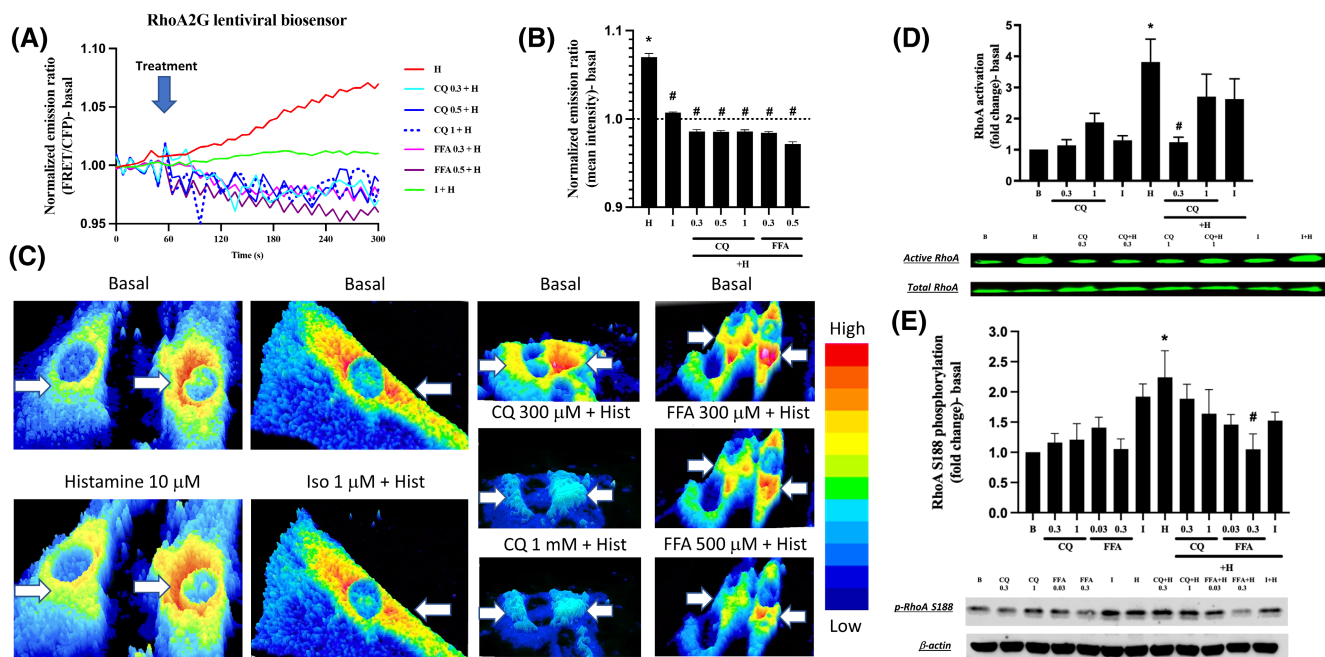


FIGURE 5 TAS2R and β_2 AR differentially regulate RhoA activity. (A and B) RhoA activity was measured in ASM cells transduced with a lentiviral FRET construct containing RhoA ($n=5-8$). Cells were treated with isoproterenol (I), chloroquine (CQ), flufenamic acid (FFA), histamine (H), or dual agonist treatment (I+H, CQ+H or FFA+H). (C) Representative images of ASM cells (4 min after treatment) with a pseudocolor lookup table. The arrows highlight areas of low or high RhoA activity as represented by fluorescent intensity. (D) Representative graph and western blot depicting the level of active RhoA “pulled down” using a GST-tagged Rhotekin RhoA-binding domain conjugated to agarose beads normalized to total RhoA in each sample ($n=3-5$). (E) Representative graph and western blot depicting phosphorylation of RhoA at residue S188 normalized to β -Actin in each sample ($n=5-6$). * $p < .05$ versus basal and # $p < .05$ versus histamine alone. Data were analyzed using a one-way ANOVA and are represented as mean \pm SEM.

3.5 | MYPT1 is differentially regulated by TAS2R agonists

MYPT1 is an important regulator of contraction, as activation of MYPT1 facilitates dephosphorylation of MLC20. It has been established that phosphorylation of MYPT1 at amino acid residues T696 and T853 leads to attenuation of MYPT1 activity, inhibiting its ability to serve as a counterbalance to MYLK.^{44–46} Therefore, levels of T696 and T853 phosphorylation were assessed in ASM cells treated with isoproterenol (1 μ M), chloroquine (300 μ M or 1 mM), or flufenamic acid (30 μ M and 300 μ M) alone, or in combination with histamine (10 μ M). There was no observed change in MYPT1 phosphorylation at amino acid residue T696 with any agonist (Figure 6A,B), but there was a significant increase in phosphorylation at residue T853 in ASM cells treated with histamine (Figure 6C,D). We observed a marked reduction in histamine-mediated T853 phosphorylation close to basal levels in ASM cells pretreated with chloroquine and flufenamic acid. Interestingly, isoproterenol inhibition of histamine-mediated MYPT1 phosphorylation at residue T853 was minimal and did not reach statistical significance. Collectively, these data suggest that chloroquine reduces histamine-mediated MLC20 phosphorylation in a RhoA- and MYPT1 T853-dependent

manner, a mechanism distinct from that employed by isoproterenol (Figure 7).

4 | DISCUSSION

Previous studies have shown that TAS2R agonists elicit bronchodilation and attenuate Gq-mediated bronchoconstriction in ASM cells and human airways in a PKA-independent manner.¹² However, TAS2R agonist mechanisms of action are unestablished. Herein, we employed a proteomics approach to delineate differences in the phosphorylation profiles of contractile-related proteins among Gq, Gs, and TAS2R signaling pathways (Figure 1). Our phosphoproteomic data reaffirmed that TAS2R signaling is mediated in a G protein- $\beta\gamma$ -dependent fashion whereas Gs signaling is not. As expected, multiple PKC substrates were significantly phosphorylated by TAS2R agonists and histamine but not isoproterenol; however, no significant GPCR-specific differences in histamine-mediated PKC substrate phosphorylation were observed (Figure 4). Interestingly, TAS2R agonist treatment was able to ablate levels of histamine-mediated RhoA activity (Figure 5) and phosphorylation of MYPT1 at the T853 residue (Figure 6) in ASM cells. Isoproterenol also inhibited

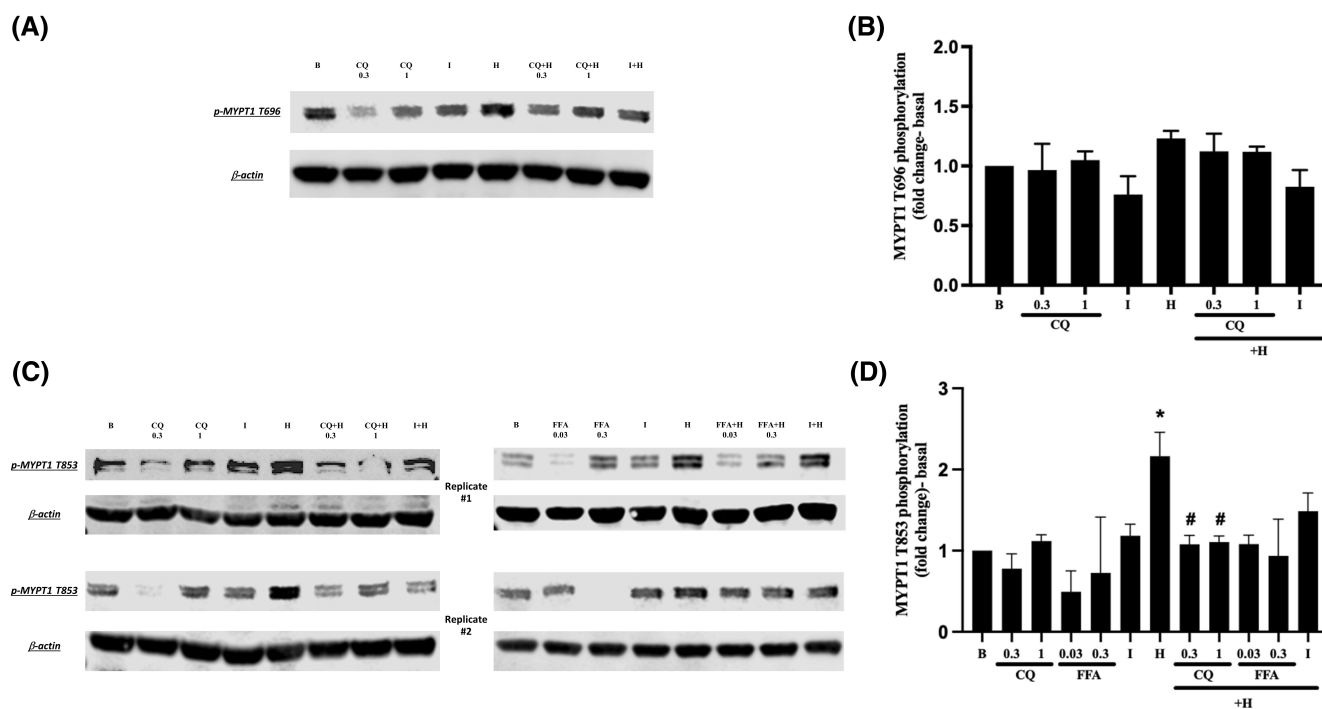


FIGURE 6 MYPT1 is differentially regulated by TAS2R and β_2 AR agonists. The phosphorylation of MYPT1 at inhibitory residues T696 and T853 was measured in ASM cells with 1 μ M isoproterenol (I), 300 μ M or 1 mM chloroquine (CQ), 30 μ M or 300 μ M flufenamic acid (FFA), 10 μ M histamine (H) or dual agonist treatment (I+H, CQ+H or FFA+H). (A) Representative western blot and graph (B) of MYPT1 T696 phosphorylation normalized to β -Actin in agonist-stimulated ASM cells ($n=4-6$). (C) Representative western blot and graph (D) of MYPT1 T853 phosphorylation normalized to β -Actin in agonist-stimulated ASM cells ($n=3-7$). * $p < .05$ versus basal and # $p < .05$ versus histamine alone. Data were analyzed using a one-way ANOVA and are represented as mean \pm SEM.

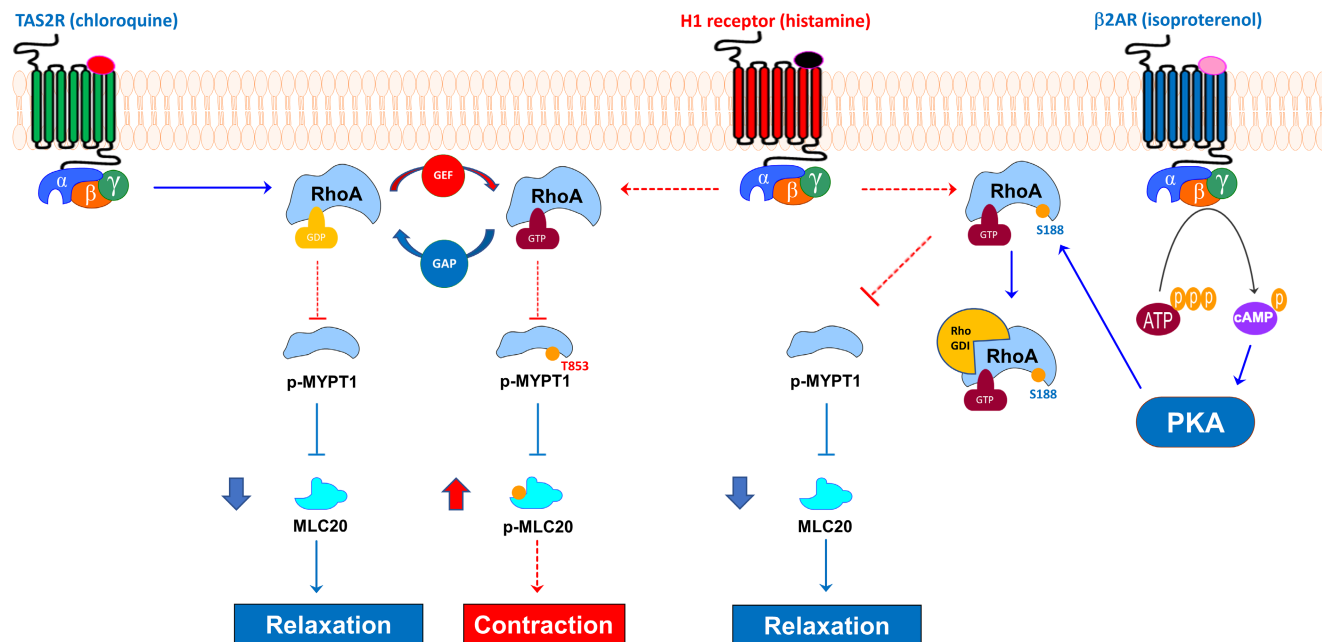


FIGURE 7 Regulation of Gq-mediated contractile proteins by TAS2R and Gs signaling. Binding of histamine to the H1 receptor leads to downstream activation of RhoA, attenuation of MYPT1, and activation of MLC20, leading to actin–myosin cross-bridge cycling and ASM contraction. Activation of the TAS2R leads to decreased RhoA activity, increased MYPT1 activity via prevention of T853 phosphorylation, and attenuation of histamine-induced MLC20 phosphorylation. Conversely, β₂AR signaling partially reduces histamine-induced MLC20 phosphorylation via PKA-mediated signaling, which partially reduces RhoA activity by phosphorylating RhoA at serine 188. This phosphorylation increases RhoA affinity for Rho-GDI, which leads to the sequestration of active GTP-bound RhoA away from the plasma membrane into the cytosol.

histamine-mediated RhoA activation and MYPT1 phosphorylation at the T853 residue, but to a lesser extent than that observed with TAS2R agonists. Furthermore, our findings suggest that isoproterenol may facilitate S188 phosphorylation of RhoA to prevent acute localization of active RhoA to the membrane, whereas histamine may induce this event to prevent any active RhoA from being degraded via the proteasome (a histamine-mediated event that was only inhibited by flufenamic acid). Although TAS2R agonists did not elicit phosphorylation of RhoA at the S188 residue as observed with individual isoproterenol treatment, flufenamic acid (300 μM) treatment appears to reduce pro-contraction histamine-mediated S188 phosphorylation of RhoA, whereas chloroquine and isoproterenol do not (Figure 5E). These findings demonstrate that GPCR-specific differences in the regulation of ASM cell tone are dependent upon differential regulation of the contractile-related proteins RhoA and MYPT1.

Rho family members are important in many cellular processes, including cell motility and contraction. Several ARHGEFs have been shown to be elevated in their expression or activity in cancer cells.^{47,48} Our data using human ASM cultures (not shown) are consistent with a prior study identifying ARHGEF12 as the most highly expressed ARHGEF in tissues obtained from severe asthma patients.⁴⁹ While individual treatment with

chloroquine (300 μM) or isoproterenol (1 μM) reduced ARHGEF12 phosphorylation and enhanced ARHGAP6 phosphorylation, only chloroquine ablated histamine-mediated ARHGEF12 phosphorylation (Figure 2). These data are consistent with immunoblot data of RhoA and MYPT1 in which we observed partial inhibition by isoproterenol (compared to complete inhibition by TAS2R agonists) of histamine-mediated activation of RhoA and MYPT1. The ARHGEF12 inhibitor Y16 has been shown to significantly reduce RhoA activity and MLC20 phosphorylation alone, or synergistically with the global RhoA inhibitor Rhosin, effects associated with inhibition of actin stress fiber formation, proliferation, and metastasis in MCF7 breast cancer cells. Specifically, Y16 reduces the interaction between ARHGEF12 and its RhoA binding pocket, most likely due to K979 and N983 residues that are uniquely conserved within the LARG GEF (including ARHGEF12) family.⁴⁷ Thus, there may be therapeutic potential for this compound as a selective inhibitor that affects ARHGEF12-RhoA binding affinity, but not the intrinsic activity of RhoA or its interactions with ARHGEFs from other families. These findings are consistent with our previous studies that isoproterenol induces ASM relaxation in a PKA-dependent manner and PKC-related proteins play an important role in TAS2R-mediated MLC20 dephosphorylation.^{7,12,50}

In addition to identifying agonist-specific regulation of RhoA-related signaling, our phosphoproteomic data also identified GPCR-specific regulation of the HIPPO signaling pathway. HIPPO signaling modulates actin cytoskeleton restructuring via changes in components such as 14-3-3 and Yes-associated protein (YAP)^{51,52}; regulation of the actin cytoskeleton plays a significant role in regulating both ASM cell contraction and proliferation.⁵³⁻⁵⁵ Rho GTPases are necessary for the nuclear localization of YAP1, where it functions as a co-activator of transcription factors driving the expression of genes important for proliferation and contraction. Gene silencing of ARHGEF12 in MCF7 breast cancer cells resulted in lower levels of YAP1 activation (*increased S127 phosphorylation*) and phalloidin-stained F-actin.⁵⁶ Moreover, activation of cofilin, a major actin cytoskeleton regulatory protein, is shown to be enhanced following TAS2R agonism, promoting F-actin destabilization and ASM cell relaxation.⁵⁷ Interestingly, PKA activity is involved in the phosphorylation of large tumor suppressor kinase (LATS), enhancing its activity to inhibit YAP1 via phosphorylation of the S381 residue.⁵⁸ Collectively, these findings suggest that HIPPO signaling may be differentially regulated by Gs-coupled and TAS2R signaling; however, the extent to which HIPPO-related effectors are differentially mediated is not fully understood.

The current study is the first to establish differences in the regulation of Gq signaling-related effector proteins between TAS2R and β_2 AR agonists. While our findings suggest that RhoA and its effectors are differentially regulated by these GPCRs, more integrative (*ex vivo*, *in vivo*) studies, employing pharmacological, molecular, or genetic targeting of effectors (including RhoA and ARHGEF12) are required to more fully establish the physiological relevance of these mechanisms. Such studies will provide further impetus for current TAS2R drug discovery efforts and substantiate the ultimate therapeutic application of TAS2R agonists in the management of obstructive pulmonary diseases.

AUTHOR CONTRIBUTIONS

DAD, MAK: Conceptualization, project administration, supervision. SC, WH, MH: Performing experiments, Data curation. SC, RBP, MAK: Manuscript writing. WH, MAK: Proteomics analysis. SC, MH, DAD, MAK, WH, RBP: Reviewing and editing the manuscript.

ACKNOWLEDGMENTS

This study was funded by the National Health Institute Grants HL137030, HL146645, HL150560, and (to D.A.D). Stanley Conaway Jr is supported by a Minority Supplement Award from NHLBI (HL137030-S1). Additional support was provided by the University of Maryland School of Pharmacy Mass Spectrometry Center (SOP1841-IQB2014).

DISCLOSURES

The Authors have no conflict of interest.

DATA AVAILABILITY STATEMENT

The data that support the findings of this study are available in the methods and results sections or in the supplemental files of this article.

ORCID

Stanley Conaway  <https://orcid.org/0000-0003-4855-6588>

Weiliang Huang  <https://orcid.org/0000-0002-9608-2172>

Miguel A. Hernandez-Lara  <https://orcid.org/0000-0002-9319-9244>

Maureen A. Kane  <https://orcid.org/0000-0002-5525-9170>

Raymond B. Penn  <https://orcid.org/0000-0001-8452-5880>

Deepak A. Deshpande  <https://orcid.org/0000-0002-6187-5332>

Deepak A. Deshpande  <https://orcid.org/0000-0002-6187-5332>

Deepak A. Deshpande  <https://orcid.org/0000-0002-6187-5332>

Deepak A. Deshpande  <https://orcid.org/0000-0002-6187-5332>

Deepak A. Deshpande  <https://orcid.org/0000-0002-6187-5332>

Deepak A. Deshpande  <https://orcid.org/0000-0002-6187-5332>

Deepak A. Deshpande  <https://orcid.org/0000-0002-6187-5332>

Deepak A. Deshpande  <https://orcid.org/0000-0002-6187-5332>

Deepak A. Deshpande  <https://orcid.org/0000-0002-6187-5332>

Deepak A. Deshpande  <https://orcid.org/0000-0002-6187-5332>

REFERENCES

- Dolhnikoff M, da Silva LF, de Araujo BB, et al. The outer wall of small airways is a major site of remodeling in fatal asthma. *J Allergy Clin Immunol*. 2009;123:1090-1097.e1.
- Gerthoffer WT, Schaafsma D, Sharma P, Ghavami S, Halayko AJ. Motility, survival, and proliferation. *Compr Physiol*. 2012;2:255-281.
- Sears MR. Adverse effects of beta-agonists. *J Allergy Clin Immunol*. 2002;110:S322-S328.
- Grove A, Lipworth BJ. Bronchodilator subsensitivity to salbutamol after twice daily salmeterol in asthmatic patients. *Lancet*. 1995;346:201-206.
- Wright JM, Smith AD, Cowan JO, Flannery EM, Herbison GP, Taylor DR. Adverse effects of short-acting beta-agonists: potential impact when anti-inflammatory therapy is inadequate. *Respirology*. 2004;9:215-221.
- Patil SB, Bitar KN. RhoA- and PKC-alpha-mediated phosphorylation of MYPT and its association with HSP27 in colonic smooth muscle cells. *Am J Physiol Gastrointest Liver Physiol*. 2006;290:G83-G95.
- Morgan SJ, Deshpande DA, Tiegs BC, et al. Beta-agonist-mediated relaxation of airway smooth muscle is protein kinase A-dependent. *J Biol Chem*. 2014;289:23065-23074.
- Einstein R, Jordan H, Zhou W, Brenner M, Moses EG, Liggett SB. Alternative splicing of the G protein-coupled receptor superfamily in human airway smooth muscle diversifies the complement of receptors. *Proc Natl Acad Sci U S A*. 2008;105:5230-5235.
- Adler E, Hoon MA, Mueller KL, Chandrashekar J, Ryba NJ, Zuker CS. A novel family of mammalian taste receptors. *Cell*. 2000;100:693-702.
- Chandrashekar J, Hoon MA, Ryba NJ, Zuker CS. The receptors and cells for mammalian taste. *Nature*. 2006;444:288-294.

11. Chandrashekar J, Mueller KL, Hoon MA, et al. T2Rs function as bitter taste receptors. *Cell*. 2000;100:703-711.
12. Deshpande DA, Wang WC, McIlmoyle EL, et al. Bitter taste receptors on airway smooth muscle bronchodilate by localized calcium signaling and reverse obstruction. *Nat Med*. 2010;16:1299-1304.
13. Meyerhof W. Elucidation of mammalian bitter taste. *Rev Physiol Biochem Pharmacol*. 2005;154:37-72.
14. Grassin-Delyle S, Abrial C, Fayad-Kobeissi S, et al. The expression and relaxant effect of bitter taste receptors in human bronchi. *Respir Res*. 2013;14:134.
15. Pulkkinen V, Manson ML, Saffholm J, Adner M, Dahlen SE. The bitter taste receptor (TAS2R) agonists denatonium and chloroquine display distinct patterns of relaxation of the Guinea pig trachea. *Am J Physiol Lung Cell Mol Physiol*. 2012;303:L956-L966.
16. Tan X, Sanderson MJ. Bitter tasting compounds dilate airways by inhibiting airway smooth muscle calcium oscillations and calcium sensitivity. *Br J Pharmacol*. 2014;171:646-662.
17. Sharma P, Yi R, Nayak AP, et al. Bitter taste receptor agonists mitigate features of allergic asthma in mice. *Sci Rep*. 2017;7:46166.
18. Zhang CH, Chen C, Lifshitz LM, Fogarty KE, Zhu MS, ZhuGe R. Activation of BK channels may not be required for bitter tastant-induced bronchodilation. *Nat Med*. 2012;18:648-650. author reply 650-641.
19. Zhang CH, Lifshitz LM, Uy KF, Ikebe M, Fogarty KE, ZhuGe R. The cellular and molecular basis of bitter tastant-induced bronchodilation. *PLoS Biol*. 2013;11:e1001501.
20. Belvisi MG, Dale N, Birrell MA, Canning BJ. Bronchodilator activity of bitter tastants in human tissue. *Nat Med*. 2011;17:776.
21. Talmon M, Rossi S, Lim D, et al. Absinthin, an agonist of the bitter taste receptor hTAS2R46, uncovers an ER-to-mitochondria Ca(2+)-shuttling event. *J Biol Chem*. 2019;294:12472-12482.
22. Panettieri RA, Murray RK, DePalo LR, Yadavish PA, Kotlikoff MI. A human airway smooth muscle cell line that retains physiological responsiveness. *Am J Phys*. 1989;256:C329-C335.
23. Guo M, Pascual RM, Wang S, et al. Cytokines regulate beta-2-adrenergic receptor responsiveness in airway smooth muscle via multiple PKA- and EP2 receptor-dependent mechanisms. *Biochemistry*. 2005;44:13771-13782.
24. Penn RB, Pascual RM, Kim YM, et al. Arrestin specificity for G protein-coupled receptors in human airway smooth muscle. *J Biol Chem*. 2001;276:32648-32656.
25. Grogan A, Huang W, Brong A, Kane MA, Kontogianni-Konstantopoulos A. Alterations in cytoskeletal and Ca(2+) cycling regulators in atria lacking the obscurin Ig58/59 module. *Front Cardiovasc Med*. 2023;10:1085840.
26. ElAli A, Hermann DM. Liver X receptor activation enhances blood-brain barrier integrity in the ischemic brain and increases the abundance of ATP-binding cassette transporters ABCB1 and ABCC1 on brain capillary cells. *Brain Pathol*. 2012;22:175-187.
27. Schoenwaelder SM, Petch LA, Williamson D, Shen R, Feng GS, Burridge K. The protein tyrosine phosphatase Shp-2 regulates RhoA activity. *Curr Biol*. 2000;10:1523-1526.
28. Ren XD, Kioussis WB, Schwartz MA. Regulation of the small GTP-binding protein rho by cell adhesion and the cytoskeleton. *EMBO J*. 1999;18:578-585.
29. Fritz RD, Letzelter M, Reimann A, et al. A versatile toolkit to produce sensitive FRET biosensors to visualize signaling in time and space. *Sci Signal*. 2013;6:rs12.
30. Elegheert J, Behiels E, Bishop B, et al. Lentiviral transduction of mammalian cells for fast, scalable and high-level production of soluble and membrane proteins. *Nat Protoc*. 2018;13:2991-3017.
31. Pertz O, Hodgson L, Klemke RL, Hahn KM. Spatiotemporal dynamics of RhoA activity in migrating cells. *Nature*. 2006;440:1069-1072.
32. Sharma P, Yadav SK, Shah SD, et al. Diacylglycerol kinase inhibition reduces airway contraction by negative feedback regulation of Gq-signaling. *Am J Respir Cell Mol Biol*. 2021;65:658-671.
33. Yadav SK, Sharma P, Shah SD, et al. Autocrine regulation of airway smooth muscle contraction by diacylglycerol kinase. *J Cell Physiol*. 2022;237:603-616.
34. Yoo EJ, Cao G, Koziol-White CJ, et al. Galpha(12) facilitates shortening in human airway smooth muscle by modulating phosphoinositide 3-kinase-mediated activation in a RhoA-dependent manner. *Br J Pharmacol*. 2017;174:4383-4395.
35. Ikebe M, Inagaki M, Kanamaru K, Hidaka H. Phosphorylation of smooth muscle myosin light chain kinase by Ca2+-activated, phospholipid-dependent protein kinase. *J Biol Chem*. 1985;260:4547-4550.
36. Gong MC, Cohen P, Kitazawa T, et al. Myosin light chain phosphatase activities and the effects of phosphatase inhibitors in tonic and phasic smooth muscle. *J Biol Chem*. 1992;267:14662-14668.
37. Kreider-Letterman G, Carr NM, Garcia-Mata R. Fixing the GAP: the role of RhoGAPs in cancer. *Eur J Cell Biol*. 2022;101:151209.
38. Rossman KL, Der CJ, Sondek J. GEF means go: turning on RHO GTPases with guanine nucleotide-exchange factors. *Nat Rev Mol Cell Biol*. 2005;6:167-180.
39. Tcherkezian J, Lamarche-Vane N. Current knowledge of the large RhoGAP family of proteins. *Biol Cell*. 2007;99:67-86.
40. Yuksel S, Aredo B, Zegeye Y, et al. Forward genetic screening using fundus spot scale identifies an essential role for Lipe in murine retinal homeostasis. *Commun Biol*. 2023;6:533.
41. Lang P, Gesbert F, Delespine-Carmagnat M, Stancou R, Pouchelet M, Bertoglio J. Protein kinase a phosphorylation of RhoA mediates the morphological and functional effects of cyclic AMP in cytotoxic lymphocytes. *EMBO J*. 1996;15:510-519.
42. Ellerbroek SM, Wennerberg K, Burridge K. Serine phosphorylation negatively regulates RhoA in vivo. *J Biol Chem*. 2003;278:19023-19031.
43. Rolli-Derkinderen M, Sauzeau V, Boyer L, et al. Phosphorylation of serine 188 protects RhoA from ubiquitin/proteasome-mediated degradation in vascular smooth muscle cells. *Circ Res*. 2005;96:1152-1160.
44. Muranyi A, Derkach D, Erdodi F, Kiss A, Ito M, Hartshorne DJ. Phosphorylation of Thr695 and Thr850 on the myosin phosphatase target subunit: inhibitory effects and occurrence in A7r5 cells. *FEBS Lett*. 2005;579:6611-6615.
45. Seko T, Ito M, Kureishi Y, et al. Activation of RhoA and inhibition of myosin phosphatase as important components in hypertension in vascular smooth muscle. *Circ Res*. 2003;92:411-418.
46. Velasco G, Armstrong C, Morrice N, Frame S, Cohen P. Phosphorylation of the regulatory subunit of smooth muscle protein phosphatase 1M at Thr850 induces its dissociation from myosin. *FEBS Lett*. 2002;527:101-104.

47. Shang X, Marchioni F, Evelyn CR, et al. Small-molecule inhibitors targeting G-protein-coupled rho guanine nucleotide exchange factors. *Proc Natl Acad Sci U S A*. 2013;110:3155-3160.
48. Vigil D, Cherfils J, Rossman KL, Der CJ. Ras superfamily GEFs and GAPs: validated and tractable targets for cancer therapy? *Nat Rev Cancer*. 2010;10:842-857.
49. Fong V, Hsu A, Wu E, et al. Arhgef12 drives IL17A-induced airway contractility and airway hyperresponsiveness in mice. *JCI Insight*. 2018;3:e123578.
50. Sharma P, Panebra A, Pera T, et al. Antimitogenic effect of bitter taste receptor agonists on airway smooth muscle cells. *Am J Physiol Lung Cell Mol Physiol*. 2016;310:L365-L376.
51. Zhou J, Xu F, Yu JJ, Zhang W. YAP is up-regulated in the bronchial airway smooth muscle of the chronic asthma mouse model. *Int J Clin Exp Pathol*. 2015;8:11132-11139.
52. Liu L, Zhai C, Pan Y, et al. Sphingosine-1-phosphate induces airway smooth muscle cell proliferation, migration, and contraction by modulating Hippo signaling effector YAP. *Am J Physiol Lung Cell Mol Physiol*. 2018;315:L609-L621.
53. Wang R, Wang Y, Liao G, et al. Abi1 mediates airway smooth muscle cell proliferation and airway remodeling via Jak2/STAT3 signaling. *iScience*. 2022;25:103833.
54. Wang Y, Liao G, Wu Y, Wang R, Tang DD. The intermediate filament protein nestin serves as a molecular hub for smooth muscle cytoskeletal signaling. *Respir Res*. 2023;24:157.
55. Li J, Wang R, Gannon OJ, et al. Polo-like kinase 1 regulates vimentin phosphorylation at Ser-56 and contraction in smooth muscle. *J Biol Chem*. 2016;291:23693-23703.
56. Lane BS, Heller B, Hollenberg MD, Wells CD. The RGS-RhoGEFs control the amplitude of YAP1 activation by serum. *Sci Rep*. 2021;11:2348.
57. Woo JA, Castano M, Kee TR, et al. A Par3/LIM kinase/cofilin pathway mediates human airway smooth muscle relaxation by TAS2R14. *Am J Respir Cell Mol Biol*. 2023;68:417-429.
58. Kim M, Kim M, Lee S, et al. Camp/PKA signalling reinforces the LATS-YAP pathway to fully suppress YAP in response to Actin cytoskeletal changes. *EMBO J*. 2013;32:1543-1555.

SUPPORTING INFORMATION

Additional supporting information can be found online in the Supporting Information section at the end of this article.

How to cite this article: Conaway S Jr, Huang W, Hernandez-Lara MA, Kane MA, Penn RB, Deshpande DA. Molecular mechanism of bitter taste receptor agonist-mediated relaxation of airway smooth muscle. *The FASEB Journal*. 2024;38:e23842. doi:[10.1096/fj.202400452R](https://doi.org/10.1096/fj.202400452R)